INTERNATIONAL JOURNAL OF REMOTE SENSING
https://doi.org/10.1080/01431161.2026.2612847

Taylor & Francis
Taylor & Francis Group

Satellite retrieval of phytoplankton size class biomass: algorithm evaluation and long-term patterns in the northern Arabian Sea

Sanjiba Kumar Baliarsingh [a], Alakes Samanta [a], P. Minu [a], S. Ayana [a,b] and Aneesh A. Lotliker [a]

[a]Indian National Centre for Ocean Information Services, Ministry of Earth Sciences, Government of India Hyderabad, India; [b]Kerala University of Fisheries and Ocean Studies, Kochi, India

ABSTRACT

Phytoplankton exist in different size classes (picophytoplankton (PP), nanophytoplankton (NP) and microphytoplankton (MP)). It's important to study the dynamics of phytoplankton size classes (PSC) for a better understanding of the characteristics and effects on the ecosystem, as they are the key drivers of the food chain and trophic pathways in the marine ecosystem. This study evaluates the performance of algorithms (Sahay, Brewin) to retrieve PSC using total chlorophyll-*a* from the Moderate Resolution Imaging Spectroradiometer onboard Aqua satellite (MODISA). The validation of satellite-derived PSC with *in situ* data showed better statistical indicators for Sahay's algorithm in retrieving PP (R^2: 0.73, slope: 0.74, intercept: 0.10, RMSE: 0.08), NP (R^2: 0.67, slope: 0.99, intercept: −.01, RMSE: 0.04), and MP (R^2: 0.76, slope: 0.81, intercept: 0.08, RMSE: 0.12). Both algorithms performed similarly for NP and MP retrievals, while Sahay's algorithm showed better accuracy for PP. Subsequently, the PSC retrieved from Sahay's algorithm was analysed to understand their spatio-temporal variability with respect to the environmental conditions. The PSC concentration varied within a year in accordance with monsoonal changes in northern Arabian Sea. The temporal variation of PSC concentration showed an inverse relationship of MP with PP, which was attributed to the nutrient availability during the period. The spatial distribution exhibited relatively higher concentrations of MP in the north during the winter monsoon (January to March) and along the western and southeastern coasts of the Arabian Sea during the summer monsoon (June to August). MP dominated the offshore northern Arabian Sea during the winter monsoon, whereas the PP exhibited higher concentration throughout the summer. The outcomes of this study highlight the strong coupling between monsoon reversal and oceanographic processes, and PSC dynamics in northern Arabian Sea.

ARTICLE HISTORY
Received 16 September 2025
Accepted 8 December 2025

KEYWORDS
Phytoplankton size class; remote sensing; Arabian Sea

CONTACT Aneesh A. Lotliker aneesh@incois.gov.in Indian National Centre for Ocean Information Services, Ministry of Earth Sciences, Government of India, Hyderabad 500090, India

1. Introduction

Phytoplankton are photoautotrophic microorganisms ubiquitous in marine environments, ranging in size from micrometre to millimetres (Bharathi, Venkataramana, and Sarma 2022; Diaz et al. 2023). Serving as primary producers in the marine environment, phytoplankton produce organic matter utilizing the sunlight that fuels the oceanic food web. In general, phytoplankton are abundant in surface waters and primarily controlled by the availability of nutrients and optimum photosynthetically active radiation (Wang et al. 2021). The spatio-temporal distribution of phytoplankton is regulated by a multitude of environmental factors, with major contributions from solar radiation, vertical mixing processes such as upwelling and downwelling, and nutrient availability (McManus and Woodson 2012). Owing to the aforementioned, any decline in phytoplankton abundance can impact the energy transfer within the ecological pyramid, from the base of the pelagic food web, and thereby can limit the growth and survival across higher trophic levels (Falkowski, Barber, and Smetacek 1998).

Spatio-temporal quantification of phytoplankton size classes provides invaluable insights to understand the biogeochemical processes underneath, aiding towards the management of higher trophic levels, including fisheries. Phytoplankton Size Classes (hereafter, PSC) play a proactive role in nutrient regulation, N_2 and carbon fixation, as well as light harvesting, thereby regulating the overall biogeochemistry and transport within the euphotic zone (Liu et al. 2018). Considering the cell size, phytoplankton are commonly classified into three categories: picophytoplankton (PP; < 2 µm), nanophytoplankton (NP; 2–20 µm), and microphytoplankton (MP; > 20 µm) (Sieburth, Smetacek, and Lenz 1978). PP account for half of the photosynthetic biomass in coastal waters as well as offshore euphotic zones (Partensky, Hess, and Vaulot 1999). NP comprises flagellates, small ciliates, and dinoflagellates. NP play a pivotal role through the food chain in the microbial loop, contributing to organic matter recycling and supporting higher trophic levels (Sherr and Sherr 2002). MP includes diatoms, cyanobacteria, and dinoflagellates (Mukherjee, Suresh, and Manna 2018). In addition, MP play an important role in new and export production. Therefore, it has been acknowledged that considering PSC is essential in understanding the oceanic biogeochemistry (Uitz et al. 2010).

Among different ocean basins, the Arabian Sea (AS) is considered one of the most productive regions, primarily attributed to the substantial nutrient enrichment from riverine/terrestrial runoff, atmospheric dust deposition, convective mixing during the winter monsoon, and lateral advection during the summer monsoon and a multitude of physical processes (Kuttippurath et al. 2023; Prakash et al. 2015; Rixen et al. 2020; Wiggert et al. 2005). With the favourable conditions of nutrient enrichment and physical mixing, this tropical basin supports a diversified phytoplankton community, which often exhibits blooms (Baliarsingh et al. 2018; Jyothibabu et al. 2015). The MP size class in northern AS is typically dominated by diatom and dinoflagellate species during the winter monsoon, and the ambient water quality, ocean dynamics, sunlight, and nutrient availability shape their abundance and community composition (Thomas 2015). The AS experiences a seasonal shift in phytoplankton community structure, as the size class distribution varies in response to environmental conditions (Ali et al. 2022; Sahay et al. 2017; Shanmugam et al. 2016). The nutrient enrichment from deep mixing favours large diatoms within the MP size class to flourish during the late winter convective phase in northeastern AS.

However, as stratification develops towards early spring, the smaller NP and PP, as well as mixotrophic dinoflagellates, such as *Noctiluca scintillans*, become more prominent, indicating the post-convective stratification of the water column and its regenerated production, which supports smaller plankton communities (Padmakumar et al. 20177). On the other hand, during the winter – spring transition, cold-core eddies in northeastern AS sustain high phytoplankton productivity through vertical nutrient supply, even after surface convection declines, thereby signifying the contribution of physical forcing in controlling PSC dynamics in this region (Smitha et al. 2022). PSC have been observed to play a significant role in the evolution cycle of algal blooms, especially in northern AS, which experiences high-biomass blooms of diatoms and dinoflagellates (dominated by *Noctiluca scintillans*) during the winter monsoon period (Albin et al. 2023; Baliarsingh et al. 2018). Even though earlier research has studied variability of PSC utilizing *in situ* data in a few open ocean pockets of northern AS, it's important to delineate the long-term patterns over the broad spatial range, which can aid in understanding environmental conduciveness for high-biomass algal blooms (Lathika 2015; Padmakumar et al. 2017; Sahay et al. 2017; Smitha et al. 2022). Recent decadal studies have demonstrated the potential of ocean colour remote sensing to characterize the PSC in the entire AS basin (Ali et al. 2022, 2025; Baliarsingh et al. 2018; Barik et al. 2020).

In the context of synoptic monitoring of marine algae, ocean colour remote sensing has been proven successful in providing critical information on the phytoplankton biomass through the retrieval of chlorophyll-*a* (henceforth chl-*a*) concentration (Kalita and Lotliker 2024). With advancements in ocean colour remote sensing, PSC concentrations are also being retrieved from satellite data, providing insights into ecosystem structure and primary production. Recent studies have further demonstrated the use of machine learning approaches for predicting seasonal and long-term changes in satellite-retrieved PSCs as well as quantifying the effect of ecological drivers (Ali et al. 2022, 2025; Brewin et al. 2010; Ciotti and Bricaud 2006; Sahay et al. 2017). Against the above backdrop, the present study was undertaken to evaluate the performance of PSC-retrieving ocean colour algorithms tailored to the AS and subsequent discerning of long-term variability of PSC with special reference to episodic high-biomass algal bloom events in northern AS.

2. Materials and methods

2.1. Study area

This study was carried out in the open ocean domain (14° to 24° N and 60° to 68°E) of the AS, covering northern, central, and some parts of the southern regions (Figure 1). The AS experiences a tropical monsoonal climate. The surface current pattern in the AS changes twice during a year due to the influence of monsoon winds. During the winter months (November to February), the wind blows from the northeast, resulting in the current flowing towards the west. The southwest monsoon winds during the summer monsoon (June to September) blow across the southern part of the AS, and an intense upwelling takes place in southeastern AS during this period (Reddy 2007). The upwelling generally prevails earlier in the southern part and gradually spreads northward along the coast of eastern AS. During the winter monsoon, relatively insignificant Ekman transport occurs in southeastern AS while convective mixing occurs in northern AS (Longhurst 2007).

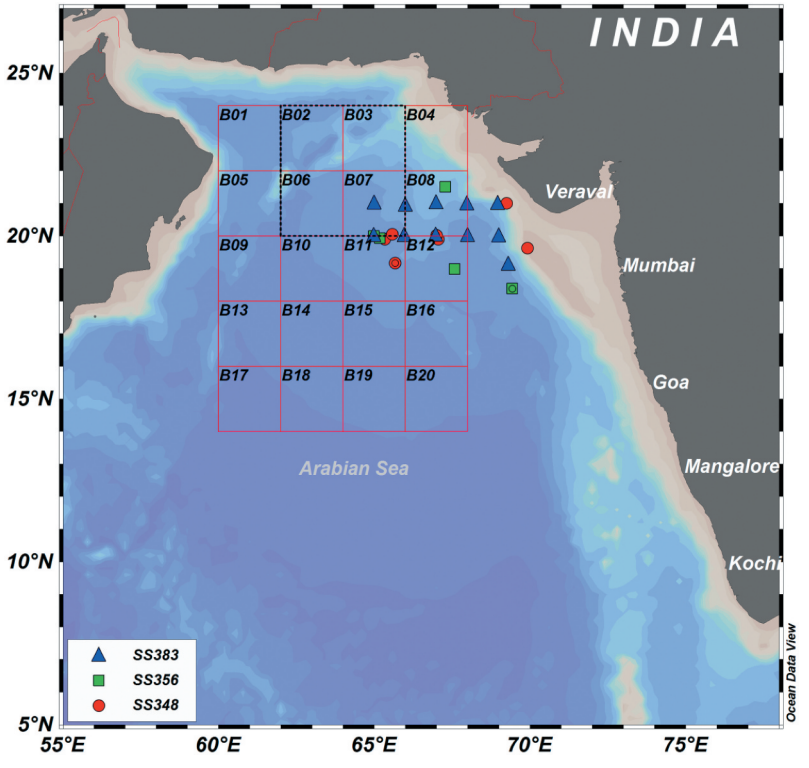

Figure 1. Map of study area. Symbols indicate *in situ* sampling stations onboard FORV Sagar Sampada cruise ID: SS383 (blue filled triangle), 356 (green filled square) and 348 (red filled circle). Northern Arabian Sea was categorized into 20 boxes (red) of 2° x 2°, where the climatological variability was analysed. The black box (20° to 24° N and 62° to 66° E) indicates the core algal bloom area.

Changes in mixed-layer depth, which are influenced by variations in surface heat flux, are the primary cause of the interannual variability of the winter algal bloom in northern AS. These variations influence nutrient transport into surface waters, which regulates the frequency and seasonality of phytoplankton blooms in this region (Keerthi et al. 2017). Governed by different ocean dynamics, southeastern AS experiences high productivity during the summer monsoon, while the same occurs in northern AS during winter (Padmakumar et al. 2017). During inter-monsoon periods, the AS becomes relatively oligotrophic (Thoppil 2023). For the ease of the present study to comprehensively cover the open ocean domain, northern AS was divided into $2° \times 2°$ boxes covering 14°-24° N latitude and 60°E- 68° E longitude (Figure 1).

2.2. Data and methodology

The *in situ* chl-*a* data used in the present study were measured during ocean expeditions onboard the research vessel FORV Sagar Sampada (cruise ID: SS348, SS356, and SS383). Water samples were collected using Niskin bottles. Filtration was carried out onboard immediately after sample collection, under subdued light conditions. PSC-fractionated chl-*a* concentration analysis for MP, NP, and PP was carried out by sequential filtration of

a known volume of water samples using filters (47 mm diameter, make: Merck-Millipore) having pore sizes 20 µm, 2 µm, and 0.2 µm (Baliarsingh et al. 2018; Brewin et al. 2014); methodological details are further elaborated in Wei et al. (2022). The residues retained on the filter paper were subjected to extraction for 24 hours in the dark and refrigerated conditions with 90% acetone. After 20 hours of extraction, the extract was centrifuged for 20 minutes at 4000 rpm. Subsequently, the spectral measurements were carried out using a UV-Visible Double Beam Spectrophotometer (Shimadzu, UV-2600), and the concentration of chl-*a* was estimated by following the protocol defined by Strickland and Parsons (1972) and as detailed in Baliarsingh et al. (2018).

Satellite-retrieved chl-*a* (4 km spatial resolution, daily) was obtained from the Moderate Resolution Imaging Spectroradiometer onboard Aqua satellite (MODISA), available at NASA's OceanColorWeb portal (https://oceancolor.gsfc.nasa.gov/). The monthly climatology was prepared from the daily data using SeaWiFS Data Analysis System (SeaDAS v7.5.1) software. The following sensor default algorithm was used for the retrieval of chl-*a* from the MODISA (Equation 1).

$$log_{10}(chl-a) = a_0 + \sum_{i=1}^{i=4} a_i \left\{ log_{10}\left[\frac{R_{rs}(\lambda_{blue})}{R_{rs}(\lambda_{green})}\right]\right\}^i \quad (1)$$

Where, $a = [0.2424, -2.7423, 1.8017, 0.0015, -1.2280]$
For MODISA, $R_{rs}(\lambda_{blue})$ is the maximum of remote sensing reflectance (R_{rs}) at wavelengths (λ) 443 and 488 nm. λ_{green} is 547 nm.

The chl-*a* concentration of different PSC, *viz*. PP, NP, and MP were retrieved using the algorithms by Sahay et al. (2017) and Brewin et al. (2010) from total chl-*a* concentration (Table 1). These abundance-based models consider total chl-*a* concentration as the combined contribution of the individual PSC, namely PP, NP, and MP. PSC algorithms were applied to MODIS-retrieved chl-*a* data, and logical expression bands were created for all different PSC using SeaDAS (version 8.1.0). The performance of the PSC-retrieval

Table 1. Model parameterization to calculate chlorophyll-*a* concentration in different size classes (pico, nano and microphytoplankton), using satellite data, provided by Brewin et al. (2010) and Sahay et al. (2017). The notations in the equations are chlorophyll-*a* concentration (C), which is the sum from pico (C_P), nano (C_N), and microphytoplankton (C_M). C_{PN}^m and C_P^m are the asymptotic maximum values that can be attained by the combination of pico and nanophytoplankton (C_{PN}) and picophytoplankton (C_P), respectively. S_{PN} and S_P are the corresponding initial slopes (adapted from Miranda et al. 2021.).

$C = C_P + C_N + C_M$
$C_{PN} = C_{PN}^m\left[1 - e^{-S_{PN}C}\right]$
$C_M = C - C_{PN}$
$C_P = C_P^m = \left[1 - e^{-S_PC}\right]$
$C_N = C_{PN} - C_P$

Parameter	Brewin et al. (2010)	Sahay et al. (2017)
C_{PN}^m	0.977	1.2330
C_P^m	0.095	0.7243
S_{PN}	0.910	0.6792
S_P	7.822	0.6645

algorithms (Brewin et al. 2010; Sahay et al. 2017) with respect to *in situ* PSC data from northern AS was evaluated by adopting a similar strategy, as followed by Miranda et al. (2021).

3. Results and discussion

3.1. Spatio-temporal variability of chlorophyll-a in the Arabian Sea

The monthly climatology maps of MODISA-chl-*a* concentration in the AS showed a clear link between high algal biomass and the monsoonal cycle (Figure 2). Higher chl-*a* concentration occurred during January to March in western as well as in northern AS. Since April, the concentration started decreasing, and May-June witnessed minimal chl-*a* in the entire basin, except for some localized areas in the coastal eastern AS. Furthermore, the chl-*a* concentration was found to increase in the southern parts and reached its maximum during September (western AS and in the coastal southeastern AS). While western Arabian Sea retained chl-*a* during October, the concentration started reducing in other areas. September had relatively higher chl-*a* levels. In the context of early monsoon months (June and July), persistent cloud cover possibly hindered satellite detection of chl-*a* signals, resulting in data gaps (Kumar et al. 2007).

During the initial phase of the winter monsoon (December), phytoplankton blooms emerge in northern AS, driven by dry northeasterly winds that enhance evaporation and surface cooling, which is also discernible in the present investigation (Figure 2). The resultant increment in surface water density promotes convective mixing, which entrains nutrients from deeper layers into the euphotic zone, supporting rapid phytoplankton growth. Biomass progressively builds through January, reaching a peak in February when mixing is intense and chl-*a* concentration is highest (Kuttippurath et al. 2023; Longhurst 2007). As the winter monsoon weakens in March, mixing declines and the nutrient supply becomes exhausted, resulting in a sharp reduction in phytoplankton biomass, with blooms persisting mainly near the coast. By April – May (inter-monsoon period), the water column becomes highly stratified due to increasing solar heating, and the absence of wind-driven mixing limits nutrient replenishment. This leads to oligotrophic conditions and relatively low productivity in the open ocean, while coastal regions show only localized patches of chl-*a*, possibly sustained by terrestrial runoff. Rising temperature also suppress the growth of some cold-adapted phytoplankton groups, thereby further lowering surface biomass in the long term (Boyce, Lewis, and Worm 2010; Poloczanska et al. 2013).

Following this nutrient-depleted phase, the onset of the southwest monsoon in June reinitiates the bloom cycle through strong coastal upwelling and basin-scale mixing, restoring nutrient levels and triggering widespread phytoplankton proliferation. The shift in monsoon winds plays a key role in controlling phytoplankton assemblages' response to changes in the mixed layer within the upwelling region. This link is so strong that any year-to-year changes in the timing or intensity of the winds are immediately mirrored in the seasonal patterns of the ecosystem (Longhurst 2007; Smith 1984). As the summer monsoon influence often extends up to October – November in northern AS, the continued nutrient supply prevents the onset of nutrient limitation, thereby sustaining

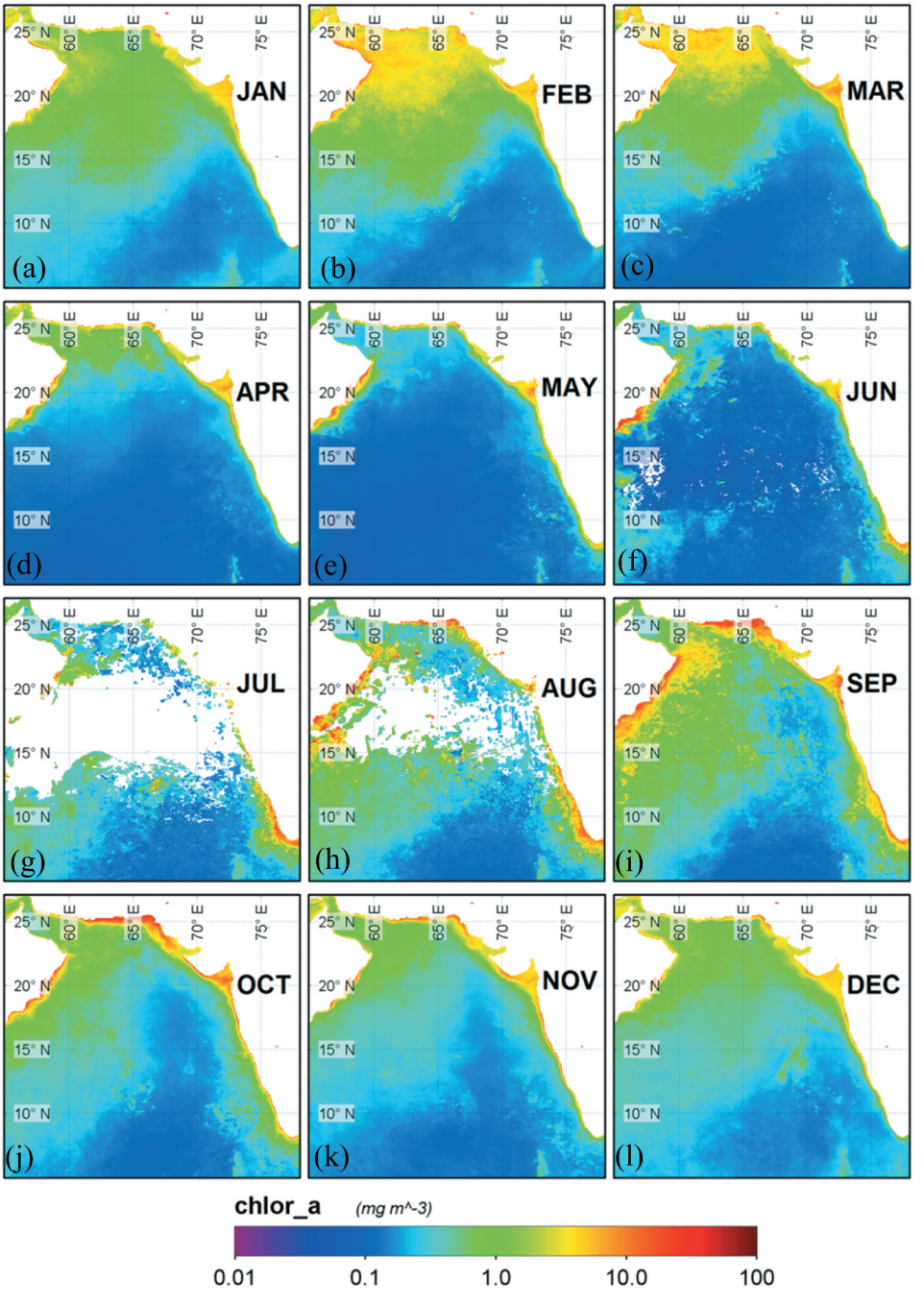

Figure 2. Spatial distribution of chlorophyll-*a* monthly climatology in the Arabian Sea.

phytoplankton proliferation even after the monsoon peak (Prakash and Ramesh 2007; Wiggert et al. 2005).

In the particular context of northern AS, the temporal variability of MODISA-retrieved chl-*a* concentration analysis focused on the 20 boxes of a 2° x 2° domain, where the

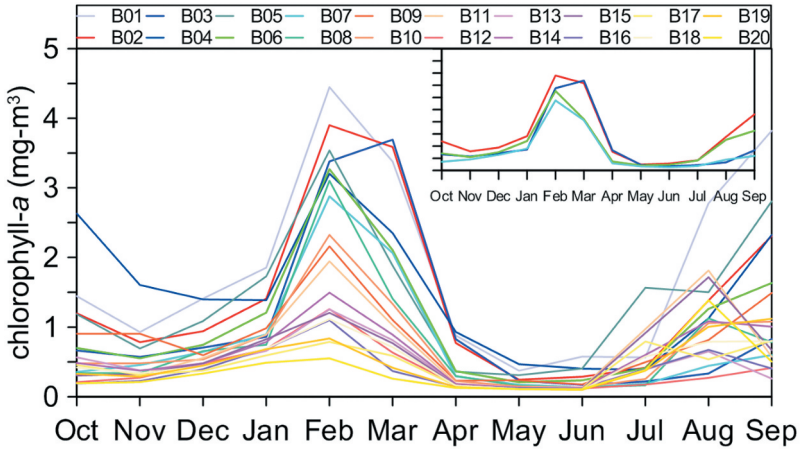

Figure 3. Temporal variability of mean chlorophyll-*a* monthly climatology in selected boxes (B01 - B10 as shown in Figure 1) in northern Arabian Sea. The inset shows the variability in boxes B02, B03, B06 and B07.

climatological variability was analysed (Figures 3 and 1). The variation indicated the extent of the high chl-*a* concentration in areas between 20°-24° N latitude to 62°-66° E longitudes (inset of Figure 3, over the 2° ×2° boxes of 2, 3, 6, and 7 as described in Figure 1). Initially, the chl-*a* concentration exhibited a gradual increase from November to January, followed by a rapid increase in February (reaching a maximum), and then started declining from March onwards. The chl-*a* reaches its minimum concentration at the end of April due to the low nutrient availability required for phytoplankton growth. This minimum is followed by a gradual increase from June onwards, extending up to September, due to the effect of the summer monsoon. The chl-*a* concentration in the majority of subsets (boxes) indicated that the highest magnitude occurs in February and the lowest in May-June, which is well aligned with episodic algal bloom phenology of northern AS (Baliarsingh et al. 2018; Lotliker et al. 2018). A concomitant recent study (Anjaneyan et al. 2023) reports initiation of winter bloom in the Gulf of Aeden (lower north-western AS) during November and lasting till February, from November to March in the Gulf of Oman (upper north-western AS), December to March in the Arabian Sea Open Waters, and from November to January in the west coast of India.

3.2. Performance of the satellite algorithms for the estimation of phytoplankton size classes

The performance of the MODISA-retrieved PSC using the two algorithms (Brewin et al. 2010; Sahay et al. 2017) was validated against the *in situ* PSC data collected from northern AS (Figure 4). The validation was further statistically analysed using slope, intercept, coefficient, root mean square error (RMSE), and absolute percentage error (APD) (Table 2). The overall statistics indicated better performance for Sahay et al. (2017) than Brewin et al. (2010). In the case of MP distribution, both models performed relatively well. For Sahay et al. (2017), the APD (33%), RMSE (0.12), and the correlation coefficient (R^2) (0.76) exhibited better values (Figure 4), whereas for Brewin et al. (2010), the APD, RMSE,

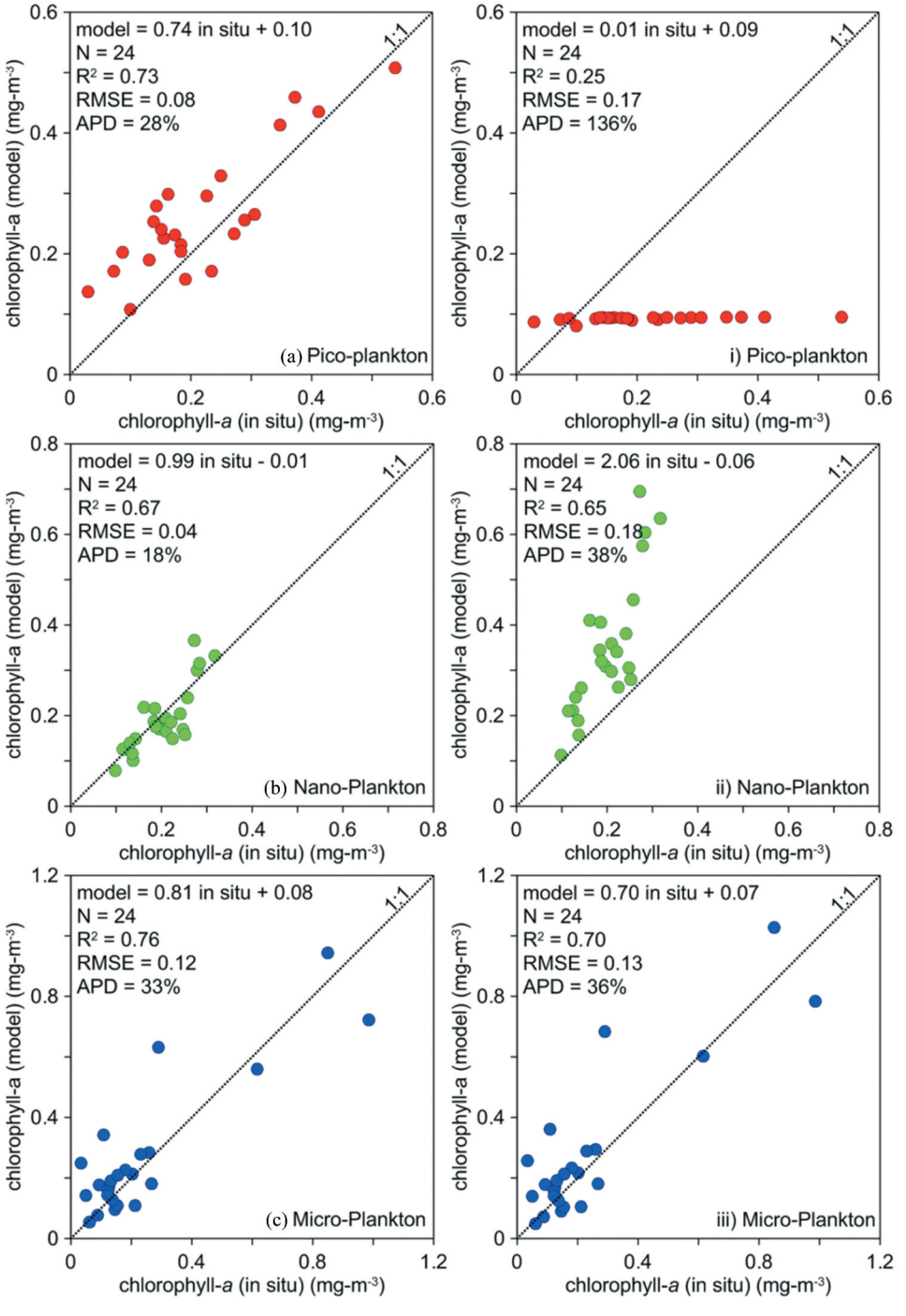

Figure 4. Scatter plot showing the relation between satellite estimate and *in situ* measured chlorophyll-*a* concentration of various phytoplankton size classes using Sahay et al. (2017) [left panel] and Brewin et al. (2010) [right panel] algorithms. The dotted line corresponds to 1:1.

Table 2. Performance indices for the relative errors between *in situ* measured and satellite estimates of chlorophyll-*a* concentration in various size classes using Sahay et al. (2017) and Brewin et al. (2010) algorithms. Statistical indices include slope (S), intercept (I), coefficient (R^2), root mean squared error (RMSE), and absolute percentage difference (APD).

Plankton	Algorithm	S	I	R^2	RMSE	APD
Picophytoplankton	Sahay	0.74	0.10	0.73	0.08	28
	Brewin	0.01	0.09	0.25	0.17	136
Nanophytoplankton	Sahay	0.99	−0.01	0.67	0.04	18
	Brewin	2.06	−0.06	0.65	0.18	38
Microphytoplankton	Sahay	0.81	0.08	0.76	0.12	33
	Brewin	0.70	0.07	0.70	0.13	36

and the coefficient values are 36%, 0.13, and 0.70, respectively (Figure 4). For NP, the APD value of Sahay et al. (2017) was 18%, RMSE 0.04, and R^2 0.60. In contrast, the APD, RMSE, and coefficient values for Brewin et al. (2010) were 38%, 0.18, and 0.65, respectively. The values generated by the algorithm of Sahay et al. (2017) are relatively near the ideal values, whereas Brewin's algorithm fell a little apart. For PP, Sahay et al. (2017) exhibited APD 28%, RMSE 0.08, and R^2 0.73; slope and intercept values were 0.74 and 0.10, respectively. In the case of Brewin's algorithm, the APD value was 136%, which exceeded the ideal value; RMSE was 0.17, which was comparatively higher than that of the Sahay et al. (2017) algorithm. The R^2 was 0.25, much lower than the ideal value of 1. The slope and intercept values were 0.01 and 0.09, respectively, indicating that the values derived from this algorithm have a widespread distribution compared to the *in situ* measured values. The results showed that the regionally tuned algorithm by Sahay et al. (2017) exhibited higher accuracy than the global model for identifying variations in the long-term patterns of PSC, especially PP, in the open ocean region of the AS. In agreement with earlier studies, this study reinforced the suitability of Sahay et al. (2017) in retrieving PSC in north Indian Ocean region (Baliarsingh et al. 2018; Barik et al. 2020; Miranda et al. 2021).

Given that the validation demonstrated the advantage of the regionally tuned algorithm by Sahay et al. (2017), it becomes necessary to situate these findings within the broader methodological framework of PSC retrieval. In this context, satellite-based approaches are generally classified into spectral-based and abundance-based methods, each suggesting distinct advantages and inherent limitations (IOCCG 2014). Spectral-based methods adopt the criteria of light absorption or scattering by phytoplankton in the ocean. Smaller cells tend to absorb blue light more strongly and show sharper absorption peaks compared to larger phytoplankton. This distinct pattern forms the foundation for classifying PSC using absorption-based techniques. In contrast, the spectral backscattering approaches consider stronger backscattering at blue wavelengths by smaller phytoplankton, while larger cells display relatively flat backscattering across the spectrum (IOCCG 2014). The advantage of spectral backscattering methods is that they are more direct, relying on distinct optical signatures, and can detect changes in PSC regardless of overall concentration. However, optical noise can affect their accuracy, limiting precise estimation under specific conditions. Variability in the optical properties of phytoplankton, driven by changes in temperature, nutrient availability, and light conditions, introduces additional uncertainties in PSC analysis (Brewin et al. 2015). The abundance-based methods estimate PSC by assuming that large cells dominate when chl-*a* concentrations are high, while small cells dominate at low chl-*a* levels. These

methods are easy to use and provide a basic idea of PSC distribution (Liu et al. 2023). In this study, two abundance-based models, *viz*. Brewin et al. (2010) and Sahay et al. (2017) have been validated for the same time period. Even though both the algorithms are abundance-based, the methodological differences in estimating *in situ* chl-*a* might have resulted in better estimation by the latter (Sahay et al. 2017).

3.3. Spatial distribution of satellite-retrieved phytoplankton size classes

Upon performance evaluation, Sahay et al. (2017) algorithm was used for PSC retrieval from MODISA and classified into PP, NP and MP, for the long-term pattern study. The monthly climatological distribution of the PSC in the AS is illustrated in Figure 5. Among the different PSC, the NP distribution appears to be uniform in the central part of the AS during May-June, with variations observed along the coastal waters due to the MP distribution existing in the region (Figure 5i-xii). The uniform distribution throughout the AS resulted from their ability to grow in optimum sunlight and the low-nutrient conditions layer (Jyothibabu et al. 2013). As the monsoon period extends, the MP concentration slowly increases, inhibiting the growth of NP. During August, September, October, and November, the NP concentration is at the lowest level in the coastal waters of southern and northern AS (Figure 5h-k). December onwards, a rapid decrease in the concentration of MP was observed in northern AS (Figure 5a-c). During this period, northern AS experiences high-biomass algal blooms dominated by *Noctiluca scintillans* (Gomes et al. 2014; Sarma et al. 2023). As the effect of the winter monsoon weakened, NP regained its ability, and an abundant as well as uniform distribution was observed in the AS during the inter-monsoon period (April-May). In corroboration with the present study, Ali et al. (2025) also reported the dominance of MP in northern AS during winter and pre-monsoon seasons, using decadal satellite data, which contributes over 50% to the total chl-*a*. In addition, the study points out that between 2010 and 2021, the MP concentration exhibited a strong decline, while PP and NP exhibited an increase attributed to the influence of sea surface temperature (SST).

During the initial period of the summer monsoon, the PP distribution was uniform and abundant in most areas of the AS (Figure 5D-G). Exceptions were observed in some parts of the north-eastern and western parts, such as the Gujarat and Somali coasts, respectively, where MP exhibited an increase. As the monsoon period extended, the MP concentration gradually increased towards the open ocean from the northwestern and north-eastern coastal regions. This period experienced a reduction in PP concentration (Figure 5H-I). During late November and early December, the concentration of MP decreased in the northern part. Conversely, the PP concentration increased in the region (Figure 5K-L). From January to early April, northern AS was observed to have a higher concentration of MP, possibly attributed to the increase in nutrients, supported by convective mixing and sufficient solar insolation penetration, favouring the blooming of the MP (Dwivedi et al. 2015; Shunmugapandi, Inamdar, and Gedam 2020). This cycle continues as the distribution of the PSC changes according to the periodic events of the AS.

Like the variability of chl-*a* in northern AS, the temporal variation of PSC indicated the higher concentration in areas between 20°-24°N latitude to 62°-66°E longitudes (over the 2° ×2° boxes of 2, 3, 6, and 7 as described in Figure 1). Therefore, subsequent analysis was

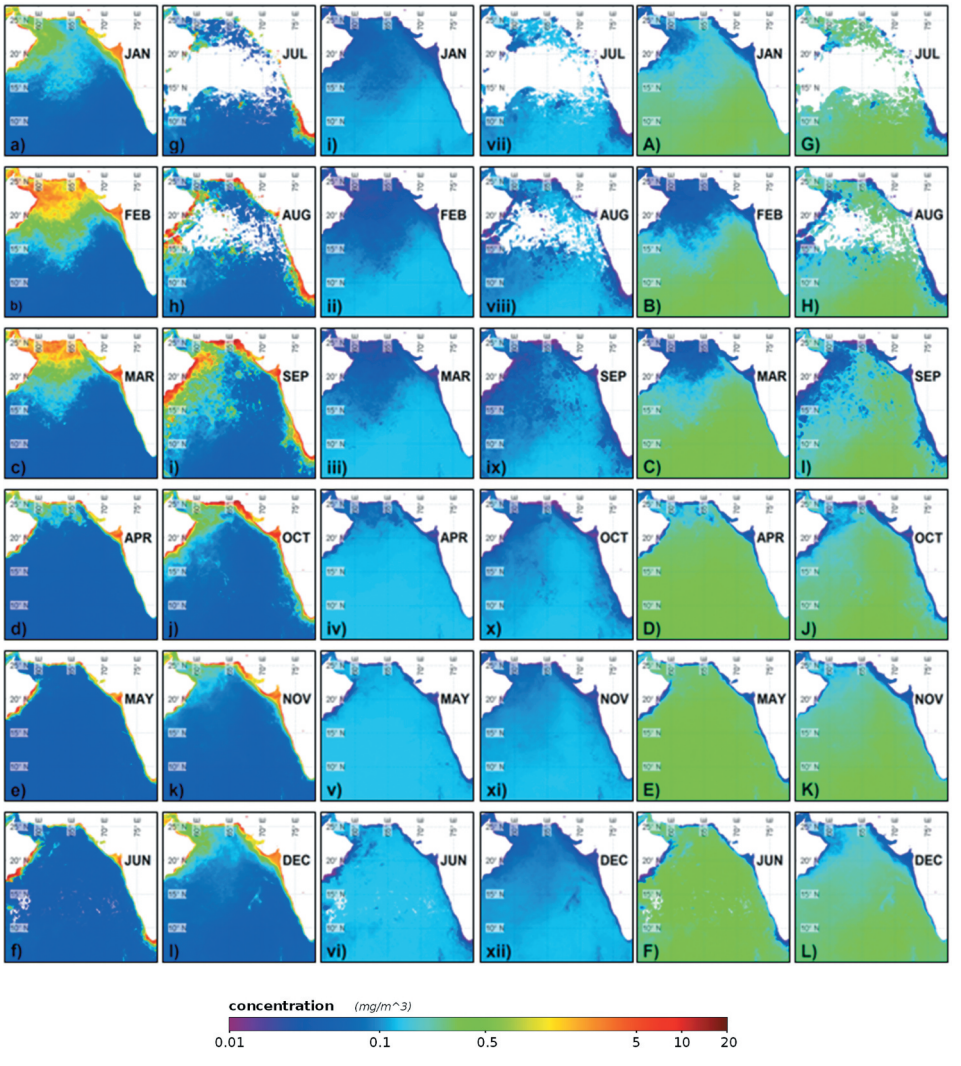

Figure 5. Monthly climatology of phytoplankton size classes fractions, in percentage, of micro (a-l), nano (i-xii) and pico-phytoplankton (A-L) derived from satellite data using Sahay et al. (2017) algorithm in the Arabian Sea.

carried out describing the fraction of chl-*a* concentration on a monthly average in PSC, averaged over the boxes 2, 3, 6 and 7 (Figure 6, boxes as defined in Figure 1) for five years (October 2013 to September 2018). The relation between the *in situ* measured fraction of chl-*a* concentration of MP and PP is illustrated in the inset of Figure 6. It can be observed that MP concentration increased during February-March, whereas the NP and PP fractions decreased, showing the inverse relationship between them. Furthermore, MP decreased from June to September, while PP and NP increased. Between PP and NP, PP was comparatively high. Earlier studies report an inverse trend between MP and PP, while NP exhibits marginal variations (Ali et al. 2025; Shunmugapandi, Gedam, and Inamdar 2022).

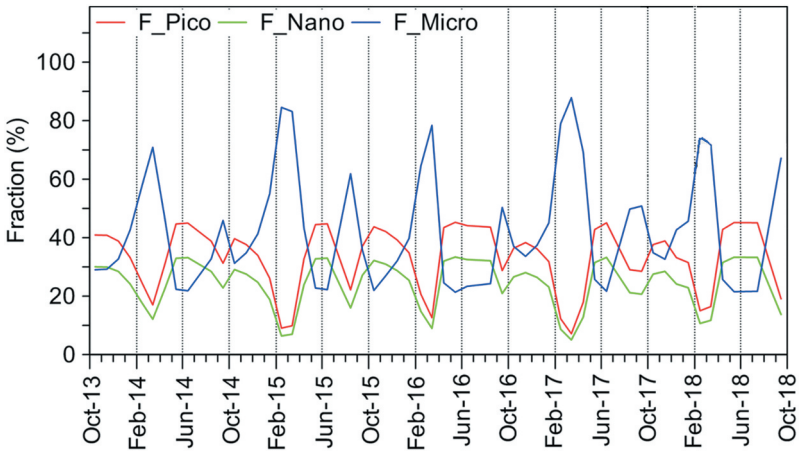

Figure 6. Fraction of monthly averaged chlorophyll-*a* concentration in phytoplankton size classes (pico, nano and micro) averaged over the boxes 2, 3, 6, and 7 (defined in Fig. 3).

The satellite-retrieved PSC concentration matched the *in situ* PSC concentration well. The variability exhibited a clear class shift from PP to NP and MP, as illustrated in Figure 5. The shift in PSC can be attributed to changes in the hydrographic conditions associated with ecosystem dynamics (Shalapyonok, Olson, and Shalapyonok 2001). The high concentration of PP in the offshore waters of northern AS during April-June can be attributed to optimum sunlight, high SST, high salinity, high nitrate, and low nutrient stoichiometry (Roy and Anil 2015). Relatively higher SST results in high stratification, leading to oligotrophic conditions where smaller PSCs only thrive (Kuttippurath et al. 2023; Shin et al. 2017). MPs, usually dominated by diatoms, prefer relatively cooler, nutrient-rich waters with moderate sunlight intensity for survival. Moreover, PP prefer low-silicate waters over diatoms. This is evidenced by the high MP in northern AS during the winter monsoon and in southeastern AS during the summer monsoon, where silicate-enriched conditions prevail (Vijayan et al. 2021).

During the winter monsoon, cool and dry winds blow from the northeast over the AS (Wiggert et al. 2000), resulting in convective mixing, which causes an increase in the mixed layer depth, allowing perturbations in the pycnocline, nitricline, and silicicline. The increased nutrients trigger MP growth and enhance productivity. While the diatoms dominate over dinoflagellates in the non-eddy areas, where convective mixing was active, dinoflagellate blooms contributed to the abundance in the periphery of the cold-core eddies (Smitha et al. 2022). The reason for the relatively large-sized dinoflagellates (i.e. mixotrophic *Noctiluca scintillans*) to proliferate in the periphery was attributed to the high salinity prevailing in the region as a result of the AS high salinity waters intrusion, along with slackened convective mixing in the periphery, resulting in low nutrient concentrations (Prasannakumar and Prasad 1999; Smitha et al. 2022). Moreover, the mean ratio of silicate/nitrate in the euphotic zone becomes lower, resulting in a 'silicate-stressed' condition for the proliferation of diatoms (Lakshmi et al. 2021). In nutrient-rich conditions, the endosymbionts of mixotrophic *Noctiluca* help the species to survive through photosynthesis, utilizing available nutrients (Manigandan et al. 2024). Once the nutrients are limited, *Noctiluca*, being a mixotroph, grazes on smaller phytoplankton, disturbing the

base of conventional food chains (Devi et al. 2021). As zooplankton do not prefer to predate on these, the abundance of *Noctiluca* at the base of the food chain represents a threat of food chain malfunction (Goes et al. 2018; Thomas, Nandan, and Padmakumar 2020).

During the summer monsoon, the high-biomass scenarios were observed along south-eastern AS. During this period, winds blow from the southeast direction, parallel to the coast, causing the warmer surface waters to be replaced by the cooler, nutrient-rich deeper waters (Narayanan et al. 2022). Additional river discharges dilute the surface waters and recharge them with nutrients. Therefore, the region becomes nutrient-rich, supporting phytoplankton growth (Figure 5). MP thrives in these regions, which are generally dominated by diatoms. In this area, there is no limitation for silicate, and the nutrient stoichiometry (Si/N, Si/P, and N/P) remains ideal for diatoms to dominate (Shah 1973).

Although this study offers useful insight into how PSCs vary across space and time in northern AS, it also has several limitations. The accuracy of PSC estimates is restricted by the assumptions built into existing classification algorithms, which may oversimplify the real optical and physiological diversity of phytoplankton communities. Satellite-based chl-*a* measurements can also be influenced by atmospheric correction issues, sensor calibration issues, and shallow light penetration in coastal waters. These factors may introduce biases in PSC estimates. In addition, gaps in satellite coverage and the lack of simultaneous *in situ* observations limit the strength of seasonal interpretations. Future research would benefit from improved algorithms tailored to regional conditions, more advanced bio-optical modelling, and expanded field campaigns that use hyperspectral sensors and autonomous platforms to enhance PSC retrievals, especially for regular operational product generation, which can aid in understanding this dynamic environment.

4. Conclusion

In conclusion, this study highlights the dynamic variability of PSC distribution in northern AS, emphasizing the strong influence of monsoonal processes on chl-*a* concentrations. The key strengths and unique contributions of this study lie in its integration of satellite-based PSC retrievals with *in situ* cruise measurements, providing a more comprehensive assessment of PSC dynamics in northern AS. The study uniquely captured spatial heterogeneity and seasonal variability in PSC distributions. This integrated approach enhances confidence in the retrieval algorithms. The application of the three-component PSC-retrieving algorithm by Sahay et al. (2017) allowed the effective retrieval of pico-, nano-, and micro-phytoplankton contributions from total chl-*a*, offering valuable insights into the ecological functioning of this region. Seasonal shifts, particularly the prominent algal blooms observed during the summer monsoon, were linked to the reversal and intensification of trade winds, subsequent Ekman transport, and upwelling processes that enrich the euphotic zone with nutrient-laden waters. These findings underscore the significance of monsoon-driven physical forcing in structuring phytoplankton communities, with potential implications for primary productivity, carbon cycling, and the broader marine food web. The salient outcomes of the present study are i) better performance of Sahay et al. (2017) algorithm in retrieving PSC from MODISA satellite data with relatively higher efficacy in retrieving PP in comparison to Brewin et al. (2010), ii) pre-dominance of MP in

northern AS during winter monsoon and along the western and south eastern coastal water of AS during summer monsoon, iii) inverse relationship of PP with MP, and iv) preponderance of PP in the open ocean waters of northern AS during summer monsoon. To improve the PSC estimations, future studies should combine extensive field measurements with longer-term time-series data, regional biogeochemistry-based bio-optical models, and higher-resolution satellite observations. For improving knowledge on ecosystem responses in the AS, the study aims at future expansion to include the effects of climate-driven changes in monsoon patterns and variability using more robust regionally tuned-validated satellite retrieval algorithms.

Acknowledgement

Authors are thankful to the Director, Indian National Centre for Ocean Information Services (INCOIS), Ministry of Earth Sciences, Government of India, Hyderabad, India, for the encouragement. The authors wish to acknowledge the NASA-GSFC for making available satellite data of MODIS-Aqua and the development team of SeaDAS. The work presented in the manuscript is a part of the doctoral research of one of the authors, S. Ayana. Grammarly™ was used as an editorial assistant to polish the language and grammar. This is INCOIS contribution no. 600.

Authors' contributions

SKB: Data curation, Formal analysis, Investigation, Writing – original draft; **AS**: Data curation, Software, Visualization, Formal analysis, Writing – original draft; **PM**: Formal analysis, Investigation, Writing – original draft; **SA**: Formal analysis, Writing – original draft. **AAL**: Conceptualization, Supervision, Resources, Data curation, Investigation, Formal analysis, Visualization, Writing – review & editing. All authors read and approved the final manuscript.

Disclosure statement

No potential conflict of interest was reported by the author(s).

Funding

The author(s) reported there is no funding associated with the work featured in this article.

ORCID

Sanjiba Kumar Baliarsingh http://orcid.org/0000-0002-9623-763X
Alakes Samanta http://orcid.org/0000-0002-6582-5850
P. Minu http://orcid.org/0000-0002-8098-5123
S. Ayana http://orcid.org/0009-0006-7282-2291
Aneesh A. Lotliker http://orcid.org/0000-0001-5467-173X

Data availability

All the data sources are well-detailed in the methodology section with the access link. The in-situ data used in this study were collected onboard the Ministry of Earth Sciences, Government of India's research vessel, FORV Sagar Sampada, under the HAB research initiative led by the Indian National

Centre for Ocean Information Services. The data can be made available upon reasonable request. Satellite-retrieved chlorophyll-*a* was obtained from the Moderate Resolution Imaging Spectroradiometer onboard Aqua satellite (MODISA), available at NASA's OceanColorWeb portal (https://oceancolor.gsfc.nasa.gov/).

References

Albin, K. J., R. Jyothibabu, S. S. Krishnan, K. T. Alok, C. K. Sherin, and G. V. M. Gupta. 2023. "Winter Phytoplankton Size Classes in the Northeastern Arabian Sea Based on In-Situ and Remote Sensing Methods." *Marine Environmental Research* 187:105972. https://doi.org/10.1016/j.marenvres.2023.105972.

Ali, S. M., A. V. Krishna, J. Kuttippurath, A. Gupta, A. Tirkey, M. Raman, and A. Sahay. 2022. "Improvement in Estimation of Phytoplankton Size Class in Arabian Sea Using Remote Sensing Measurements." *IEEE Transactions on Geoscience and Remote Sensing* 60:1–12. https://doi.org/10.1109/TGRS.2022.3223161.

Ali, S. M., J. Kuttippurath, A. V. Krishna, A. Gupta, D. Ganguly, M. Raman, A. Sahay, and K. N. Babu. 2025. "An In-Depth Analysis of the Impact of Environmental Drivers on the Variability of Phytoplankton Community in the Arabian Sea During 2010–2021." *Environmental Science: Processes & Impacts* 27 (2): 498–512.

Anjaneyan, P., J. Kuttippurath, P. H. Kumar, S. M. Ali, and M. Raman. 2023. "Spatio-Temporal Changes of Winter and Spring Phytoplankton Blooms in Arabian Sea During the Period 1997–2020." *Journal of Environmental Management* 332:117435. https://doi.org/10.1016/j.jenvman.2023.117435.

Baliarsingh, S. K., A. A. Lotliker, V. Sudheesh, A. Samanta, S. Das, and A. K. Vijayan. 2018. "Response of Phytoplankton Community and Size Classes to Green Noctiluca Bloom in the Northern Arabian Sea." *Marine Pollution Bulletin* 129 (1): 222–230. https://doi.org/10.1016/j.marpolbul.2018.02.031 .

Barik, K. K., S. K. Baliarsingh, A. K. Jena, S. Srichandan, A. Samanta, and A. A. Lotliker. 2020. "Satellite Retrieved Spatio-Temporal Variability of Phytoplankton Size Classes in the Arabian Sea." *Journal of the Indian Society of Remote Sensing* 48 (10): 1413–1419. https://doi.org/10.1007/s12524-020-01165-w.

Bharathi, M. D., V. Venkataramana, and V. V. S. S. Sarma. 2022. "Phytoplankton Community Structure is Governed by Salinity Gradient and Nutrient Composition in the Tropical Estuarine System." *Continental Shelf Research* 234:104643. https://doi.org/10.1016/j.csr.2021.104643.

Boyce, D. G., M. R. Lewis, and B. Worm. 2010. "Global Phytoplankton Decline Over the Past Century." *Nature* 466 (7306): 591–596. https://doi.org/10.1038/nature09268.

Brewin, R. J., S. Sathyendranath, T. Jackson, R. Barlow, V. Brotas, R. Airs, and T. Lamont. 2015. "Influence of Light in the Mixed-Layer on the Parameters of a Three-Component Model of Phytoplankton Size Class." *Remote Sensing of Environment* 168:437–450. https://doi.org/10.1016/j.rse.2015.07.004.

Brewin, R. J., S. Sathyendranath, P. K. Lange, and G. Tilstone. 2014. "Comparison of Two Methods to Derive the Size-Structure of Natural Populations of Phytoplankton." *Deep Sea Research Part I: Oceanographic Research Papers* 85:72–79. https://doi.org/10.1016/j.dsr.2013.11.007.

Brewin, R. J. W., S. Sathyendranath, T. Hirata, S. J. Lavender, R. M. Barciela, and N. J. Hardman-Mountford. 2010. "A Three-Component Model of Phytoplankton Size Class for the Atlantic Ocean." *Ecological Modelling* 221 (11): 1472–1483. https://doi.org/10.1016/j.ecolmodel.2010.02.014.

Ciotti, A. M., and A. Bricaud. 2006. "Phytoplankton Size Structure and Primary Production in the Ocean from Space: Recent Advances and Perspectives." *Remote Sensing of Environment* 102 (1–2): 23–38.

Devi, C. A., K. G. Vimalkumar, K. B. Padmakumar, C. T. Lathika, T. P. Maneesh, and M. Sudhakar. 2021. "Understanding the Microzooplankton Mediated Food Web of the Winter–Spring Noctiluca Bloom in the Northeastern Arabian Sea Ecosystem." *Regional Studies in Marine Science* 42:101623. https://doi.org/10.1016/j.rsma.2021.101623.

Diaz, B. P., E. Zelzion, K. Halsey, P. Gaube, M. Behrenfeld, and K. D. Bidle. 2023. "Marine Phytoplankton Downregulate Core Photosynthesis and Carbon Storage Genes Upon Rapid Mixed Layer Shallowing." *The ISME Journal* 17 (7): 1074–1088. https://doi.org/10.1038/s41396-023-01416-x.

Dwivedi, R., M. Rafeeq, B. R. Smitha, K. B. Padmakumar, L. C. Thomas, V. N. Sanjeevan, P. Prakash, and M. Raman. 2015. "Species Identification of Mixed Algal Bloom in the Northern Arabian Sea Using Remote Sensing Techniques." *Environmental Monitoring and Assessment* 187 (2): 51. https://doi.org/10.1007/s10661-015-4291-2.

Falkowski, P. G., R. T. Barber, and V. Smetacek. 1998. "Biogeochemical Controls and Feedbacks on Ocean Primary Production." *Science* 281 (5374): 200–206. https://doi.org/10.1126/science.281.5374.200.

Goes, J. I., H. D. R. Gomes, K. Al-Hashimi, and A. Buranapratheprat. 2018. "Ecological Drivers of Green Noctiluca Blooms in Two Monsoonal-Driven Ecosystems." In *Global Ecology and Oceanography of Harmful Algal Blooms*, edited by P. Gilbert, E. Berdalet, M. Burford, G. Pitcher, and M. Zhou, 327–336. Cham: Springer International Publishing.

Gomes, H. D. R., I. Joaquim, S. G. P. Matondkar, E. J. Buskey, S. Basu, S. Parab, and P. Thoppil. 2014. "Massive Outbreaks of *Noctiluca Scintillans* Blooms in the Arabian Sea Due to Spread of Hypoxia." *Nature Communications* 5 (1): 4862. https://doi.org/10.1038/ncomms5862.

IOCCG. 2014. *Phytoplankton Functional Types from Space*. Edited by S. Sathyendranath, 154. Dartmouth, NS, Canada: International Ocean-Colour Coordinating Group (IOCCG). http://dx.doi.org/10.25607/OBP-1.

Jyothibabu, R., A. P. Mohan, L. Jagadeesan, A. Anjusha, K. R. Muraleedharan, K. R. Lallu, K. Kiran, and N. Ullas. 2013. "Ecology and Trophic Preference of Picoplankton and Nanoplankton in the Gulf of Mannar and the Palk Bay, Southeast Coast of India." *Journal of Marine Systems* 111:29–44. https://doi.org/10.1016/j.jmarsys.2012.09.006.

Jyothibabu, R., P. N. Vinayachandran, N. V. Madhu, R. S. Robin, C. Karnan, L. Jagadeesan, and A. Anjusha. 2015. "Phytoplankton Size Structure in the Southern Bay of Bengal Modified by the Summer Monsoon Current and Associated Eddies: Implications on the Vertical Biogenic Flux." *Journal of Marine Systems* 143:98–119. https://doi.org/10.1016/j.jmarsys.2014.10.018.

Kalita, R., and A. A. Lotliker. 2024. "Assessment of Satellite-Based Net Primary Productivity Models in Different Biogeochemical Provinces Over the Northern Indian Ocean." *International Journal of Remote Sensing* 45 (23): 8807–8826. https://doi.org/10.1080/01431161.2023.2247533.

Keerthi, M. G., M. Lengaigne, M. Levy, J. Vialard, V. Parvathi, C. de Boyer Montégut, C. Ethé, et al. 2017. "Physical Control of Interannual Variations of the Winter Chlorophyll Bloom in the Northern Arabian Sea." *Biogeosciences* 14 (15): 3615–3632. https://doi.org/10.5194/bg-14-3615-2017.

Kumar, S. P., M. Nuncio, N. Ramaiah, S. Sardessai, J. Narvekar, V. Fernandes, and J. T. Paul. 2007. "Eddy-Mediated Biological Productivity in the Bay of Bengal During Fall and Spring Intermonsoons." *Deep Sea Research Part I: Oceanographic Research Papers* 54 (9): 1619–1640.

Kuttippurath, J., S. Maishal, P. Anjaneyan, N. Sunanda, and K. Chakraborty. 2023. "Recent Changes in Atmospheric Input and Primary Productivity in the North Indian Ocean." *Heliyon* 9 (7): e17940. https://doi.org/10.1016/j.heliyon.2023.e17940.

Lakshmi, R. S., S. Prakash, A. A. Lotliker, S. K. Baliarsingh, A. Samanta, T. Mathew, A. Chatterjee B. K. Sahuand , T. B. Nair. 2021. "Physicochemical Controls on the Initiation of Phytoplankton Bloom During the Winter Monsoon in the Arabian Sea." *Scientific Reports* 11 (1): 13448.

Lathika, C. T. 2015. "Microphytoplankton Community Structure along the North Eastern Arabian Sea during Winter Monsoon." Ph.D Thesis, Cochin University of Science and Technology, 218.

Liu, Q., S. Kandasamy, B. Lin, H. Wang, and C. T. A. Chen. 2018. "Biogeochemical Characteristics of Suspended Particulate Matter in Deep Chlorophyll Maximum Layers in the Southern East China Sea." *Biogeosciences* 15 (7): 2091–2109. https://doi.org/10.5194/bg-15-2091-2018.

Liu, X., J. Sun, Y. Wei, and Y. Liu. 2023. "Relationship Between Cell Volume and Particulate Organic Matter for Different Size Phytoplankton." *Marine Pollution Bulletin* 194:115298. https://doi.org/10.1016/j.marpolbul.2023.115298.

Longhurst, A. 2007. *Ecological Geography of the Sea*. 2nd ed. Elsevier.

Lotliker, A. A., S. K. Baliarsingh, V. L. Trainer, M. L. Wells, C. Wilson, T. U. Bhaskar, A. Samanta, and S. R. Shahimol. 2018. "Characterization of Oceanic Noctiluca Blooms Not Associated with Hypoxia

in the Northeastern Arabian Sea." *Harmful Algae* 74:46–57. https://doi.org/10.1016/j.hal.2018.03.008.

Manigandan, V., C. Muthukumar, C. Shah, N. Logesh, S. K. Sivadas, K. Ramu, and M. R. Murthy. 2024. "Phylogenetic Affiliation of Pedinomonas noctilucae and Green Noctiluca scintillans Nutritional Dynamics in the Gulf of Mannar, Southeastern Arabian Sea." *Protist* 175 (2): 126019. https://doi.org/10.1016/j.protis.2024.126019.

McManus, M. A., and C. B. Woodson. 2012. "Plankton Distribution and Ocean Dispersal." *Journal of Experimental Biology* 215 (6): 1008–1016.

Miranda, J., A. A. Lotliker, S. K. Baliarsingh, A. K. Jena, A. Samanta, K. C. Sahu, and T. S. Kumar. 2021. "Satellite Estimates of the Long-Term Trend in Phytoplankton Size Classes in the Coastal Waters of North-western Bay of Bengal." *Oceanologia* 63 (1): 40–50. https://doi.org/10.1016/j.oceano.2020.09.003.

Mukherjee, M., V. R. Suresh, and R. K. Manna. 2018. "Microplankton Dynamics of a Coastal Lagoon, Chilika: Interactive Effect of Environmental Parameters on Microplankton Groups." *Environmental Monitoring and Assessment* 190 (11): 689. https://doi.org/10.1007/s10661-018-7049-9.

Narayanan, N. S. V., C. V. Ramu, K. Rasheed, Y. V. B. Sarma, and G. V. M. Gupta. 2022. "Observational Evidence on the Coastal Upwelling Along the Northwest Coast of India During Summer Monsoon." *Environmental Monitoring and Assessment* 194 (1): 5. https://doi.org/10.1007/s10661-021-09659-x.

Padmakumar, K. B., L. C. Thomas, K. G. Vimalkumar, C. R. Asha Devi, T. P. Maneesh, A. Vijayan, G. V. M. Gupta, and M. Sudhakar. 2017. "Hydrobiological Responses of the North Eastern Arabian Sea During Late Winter and Early Spring Inter-Monsoons and the Repercussions on Open-Ocean Blooms." *Journal of the Marine Biological Association of the United Kingdom* 97 (7): 1467–1478. https://doi.org/10.1017/S0025315416000795.

Partensky, F., W. R. Hess, and D. Vaulot. 1999. "Prochlorococcus, a Marine Photosynthetic Prokaryote of Global Significance." *Microbiology and Molecular Biology Reviews* 63 (1): 106–127. https://doi.org/10.1128/MMBR.63.1.106-127.1999.

Poloczanska, E. S., C. J. Brown, W. J. Sydeman, W. Kiessling, D. S. Schoeman, P. J. Moore, K. Brander, et al. 2013. "Global Imprint of Climate Change on Marine Life." *Nature Climate Change* 3 (10): 919–925. https://doi.org/10.1038/nclimate1958.

Prakash, S., and R. Ramesh. 2007. "Is the Arabian Sea Getting More Productive?" *Current Science* 92 (5): 667–671.

Prakash, S., R. Ramesh, M. S. Sheshshayee, R. Mohan, and M. Sudhakar. 2015. "Nitrogen Uptake Rates and F-Ratios in the Equatorial and Southern Indian Ocean." *Current Science* 108 (2): 239–245.

Prasannakumar, S., and T. G. Prasad. 1999. "Formation and Spreading of Arabian Sea High-Salinity Water Mass." *Journal of Geophysical Research: Oceans* 104 (C1): 1455–1464. https://doi.org/10.1029/1998JC900022.

Reddy, M. 2007. *Ocean Environment and Fisheries*. CRC Press.

Rixen, T., G. Cowie, B. Gaye, J. Goes, H. do Rosário Gomes, R. R. Hood, Z. Lachkar, H. Schmidt, J. Segschneider, and A. Singh. 2020. "Reviews and syntheses: Present, past, and future of the oxygen minimum zone in the northern Indian Ocean." *Biogeosciences* 17 (23): 6051–6080.

Roy, R., and A. C. Anil. 2015. "Complex interplay of physical forcing and Prochlorococcus population in ocean." *Progress in Oceanography* 137:250–260.

Sahay, R., S. M. Ali, A. Gupta, and J. I. Goes. 2017. "Ocean Color Satellite Determination of Phytoplankton Size Classes in the Arabian Sea During Winter Monsoon." *Remote Sensing of Environment* 198:286–296.

Sarma, N. S., S. K. Baliarsingh, A. A. Lotliker, S. R. Pandi, A. Samanta, and S. Srichandan. 2023. "Sea Surface Temperature and Phytoplankton Abundance as Crucial Proxies for Green Noctiluca Bloom Monitoring in the Northeastern Arabian Sea: A Case Study." *Ocean Science Journal* 58 (1): 2. https://doi.org/10.1007/s12601-022-00096-6.

Shah, N. 1973. "Seasonal Variation of Phytoplankton Pigments in the Laccadive Sea Off Cochin." In *The Biology of the Indian Ocean*, edited by B. Zeitzschel, and S. A. Gerlach, 175–185.

Shalapyonok, A., R. J. Olson, and L. S. Shalapyonok. 2001. "Arabian Sea phytoplankton during Southwest and Northeast Monsoons 1995: composition, size structure and biomass from

individual cell properties measured by flow cytometry." *Deep-Sea Research Part II: Topical Studies in Oceanography* 48 (6–7): 1231–1261.

Shanmugam, P., T. Varunan, S. N. Nagendra Jaiganesh, A. Sahay, and P. Chauhan. 2016. "Optical Assessment of Coloured Dissolved Organic Matter and Its Related Parameters in Dynamic Coastal Water Systems." *Estuarine, Coastal and Shelf Science* 175:126–145. https://doi.org/10.1016/j.ecss.2016.03.020.

Sherr, E. B., and B. F. Sherr. 2002. "Significance of Predation by Protists in Aquatic Microbial Food Webs." *Antonie Van Leeuwenhoek* 81 (1–4): 293–308. https://doi.org/10.1023/A:1020591307260.

Shin, J. W., J. Park, J. G. Choi, Y. H. Jo, J. J. Kang, H. Joo, and S. H. Lee. 2017. "Variability of Phytoplankton Size Structure in Response to Changes in Coastal Upwelling Intensity in the Southwestern East Sea." *Journal of Geophysical Research: Oceans* 122 (12): 10262–10274. https://doi.org/10.1002/2017JC013467.

Shunmugapandi, R., S. Gedam, and A. B. Inamdar. 2022. "Impact of Indian Ocean Dipole Events on Phytoplankton Size Classes Distribution in the Arabian Sea." *Oceans* 3 (4): 480–493. https://doi.org/10.3390/oceans3040032.

Shunmugapandi, R., A. B. Inamdar, and S. K. Gedam. 2020. "Long-Time-Scale Investigation of Phytoplankton Communities Based on Their Size in the Arabian Sea." *International Journal of Remote Sensing* 41 (15): 5992–6009. https://doi.org/10.1080/01431161.2020.1714785.

Sieburth, J. M., V. Smetacek, and J. Lenz. 1978. "Pelagic Ecosystem Structure: Heterotrophic Compartments of the Plankton and Their Relationship to Plankton Size Fractions 1." *Limnology and Oceanography* 23 (6): 1256–1263. https://doi.org/10.4319/lo.1978.23.6.1256.

Smith, S. L. 1984. "Biological Indications of Active Upwelling in Northwest Indian Ocean in 1964 and 1979, and a comparison with Peru and northwest Africa." *Deep Sea Research Part A. Oceanographic Research Papers* 13 (6–8): 951–967. https://doi.org/10.1016/0198-0149(84)90050-5.

Smitha, B. R., V. N. Sanjeevan, K. B. Padmakumar, M. S. Hussain, T. C. Salini, and J. K. Lix. 2022. "Role of Mesoscale Eddies in the Sustenance of High Biological Productivity in North Eastern Arabian Sea During the Winter-Spring Transition Period." *Science of the Total Environment* 809: 151173.

Strickland, J. D. H., and T. R. Parsons. 1972. *A Practical Handbook of Seawater Analysis*, 1–310. 2nd ed. Vol. 167. Ottawa, Canada: Fisheries Research Board of Canada.

Thomas, L. C. 2015. "Microphytoplankton Community Structure in the North Eastern Arabian Sea During Winter Monsoon." Doctoral dissertation, Kochi, India: Cochin University of Science and Technology.

Thomas, L. C., S. B. Nandan, and K. B. Padmakumar. 2020. "Understanding the Dietary Relationship Between Extensive Noctiluca Bloom Outbreaks and Jellyfish Swarms Along the Eastern Arabian Sea (West Coast of India)." *Indian Journal of Geo Marine Sciences* 49 (8): 1389–1394.

Thoppil, P. G. 2023. "Enhanced Phytoplankton Bloom Triggered by Atmospheric High-Pressure Systems Over the Northern Arabian Sea." *Scientific Reports* 13 (1): 769. https://doi.org/10.1038/s41598-023-27785-z.

Uitz, J., H. Claustre, B. Gentili, and D. Stramski. 2010. "Phytoplankton Class-Specific Primary Production in the World's Oceans: Seasonal and Interannual Variability from Satellite Observations." *Global Biogeochemical Cycles* 24 (3). https://doi.org/10.1029/2009GB003680.

Vijayan, A. K., B. B. Reddy, V. Sudheesh, P. H. Marathe, V. N. Nampoothiri, N. V. Harikrishnachari, P. Kavya, G. V. M. Gupta, and M. V. Ramanamurthy. 2021. "Phytoplankton Community Structure in a Contrasting Physico-Chemical Regime Along the Eastern Arabian Sea During the Winter Monsoon." *Journal of Marine Systems* 215:103501. https://doi.org/10.1016/j.jmarsys.2020.103501.

Wang, Y., J. Kang, X. Sun, J. Huang, Y. Lin, and P. Xiang. 2021. "Spatial Patterns of Phytoplankton Community and Biomass Along the Kuroshio Extension and Adjacent Waters in Late Spring." *Marine Biology* 168 (3): 40. https://doi.org/10.1007/s00227-021-03846-7.

Wei, Y., Z. Cui, X. Wang, G. Teng, K. Qu, and J. Sun. 2022. "Comparative Analysis of Total and Size-Fractionated Chlorophyll a in the Yellow Sea and Western Pacific." *Frontiers in Microbiology* 13:903159. https://doi.org/10.3389/fmicb.2022.903159.

Wiggert, J. D., R. R. Hood, K. Banse, and J. C. Kindle. 2005. "Monsoon-Driven Biogeochemical Processes in the Arabian Sea." *Progress in Oceanography* 65 (2–4): 176–213. https://doi.org/10.1016/j.pocean.2005.03.008.

Wiggert, J. D., B. H. Jones, T. D. Dickey, K. H. Brink, R. A. Weller, J. Marra, and L. A. Codispoti. 2000. "The Northeast Monsoon's Impact on Mixing, Phytoplankton Biomass, and Nutrient Cycling in the Arabian Sea." *Deep-Sea Research Part II: Topical Studies in Oceanography* 47 (7–8): 1353–1385.